

# Development, Optimization, and Design for Robustness of a Novel FMVSS 201U Energy Absorber

David M. Fox

*US Army Tank Automotive Research, Development and Engineering Center  
Warren, MI*

## Abstract

*In order to streamline the product development process, the design space for FMVSS 201U impact performance of a steel mechanical energy absorber assembly was investigated by means of LS-DYNA 970 explicit finite element simulation methods in conjunction with statistical analytical procedures. A sequence of response surfaces, based on various levels of design parameters, was developed and used to determine minimal stopping distance for which it would be possible to achieve acceptable impact attenuation performance under various impact loading conditions given a worst case assumption of rigid vehicle interior body panels. A model was also developed, based on the variation of deterministic variables, in order to estimate and minimize, by means of a robustness analysis, the range of deviation of product response that would be expected as a result of variability in manufacturing and installation processes.*

## Introduction

Various motor vehicles have been constructed with relatively rigid body panels and various other types of interior assembly that offer opportunities for reduction of the incidence and severity of head injury by means of appropriately designed energy absorbing devices. The general performance of one such device, a steel assembly utilizing plastic deformation of fins and a cover sheet to reduce impact severity when mounted on rigid body panels, was previously investigated via simulation studies and it was determined that this type of absorber might be a worthwhile candidate for application to the solution of some of these types of problem [1].

As a continuation of that work, the successive response surface method (SRSM) of Stander and Craig [2] was here used to determine the characteristics of a design that would allow minimization of the crush space required to enable acceptably low levels of impact severity.

Classical factorial design techniques were used to investigate impact response robustness in the vicinity of the optimum combination of design variable settings. It was found that a small change in the prescribed center point of one of the design variables would enable a significant improvement in the robustness of the design.

## Energy Absorber Design and Simulation

The energy absorber system, which was simulated using LS-DYNA explicit finite element analysis code [3], is illustrated in Figure 1 and was comprised of a network of 0.5 inch wide mild steel fins that were sandwiched between a rigid panel and a mild steel surface panel shell. Each fin had a 0.25 inch tab at each end for use as an attachment to the surface and rigid body panels. The fin tabs were connected to one another by means of a mild steel web with a view toward ensuring proper fin alignment during manufacture, assembly, and installation. The fin / web

assembly was connected to the cover sheet via spot welds and was constrained at the rigid panel end using single point constraints. For the purposes of this study absorber impact performance was adjusted by varying crush space, spacing distance between fins, and the thickness of fins, webs, and cover sheet.

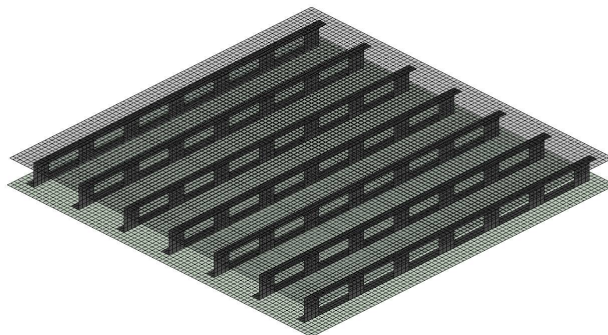


Figure 1. Metal fin impact energy absorber.

Component level impact test simulations were performed with the intent of modeling what would be expected to occur during US Federal Motor Vehicle Safety Standard (FMVSS) 201U upper interior tests [4]. All impact simulations involved the use of a validated First Technology Safety Systems free motion headform finite element model. A free motion headform is a modified anthropometric test device (crash dummy) head that is instrumented with a tri-axial accelerometer in order to measure acceleration during the course of impact.

The acceleration history from each impact was used to calculate a quantity defined as the head injury criterion (HIC) according to Equation (1), where  $a(t)$  is defined as the resultant acceleration as a function of time;  $t_1$  and  $t_2$  are any two points in time during the impact separated by not more than 36 milliseconds.  $HIC(d)$  is a correlation between HIC for the free motion headform and HIC for a full 50th percentile dummy and is calculated according to Equation (2). Lower HIC is better, FMVSS 201U requires that  $HIC(d)$  be less than 1000.

For all simulations, the free motion headform impacted the energy absorber with an initial

$$HIC = \max_{t_1, t_2} \left\{ \left[ \frac{\int_{t_1}^{t_2} a(\tau) d\tau}{(t_2 - t_1)} \right]^{2.5} (t_2 - t_1) \right\} \tag{1}$$

$$HIC(d) = 0.75446 (HIC) + 166.4 \tag{2}$$

velocity of 15 mph and the velocity vector of the head at impact was at a 20° angle with the normal to the cover surface. Figure 2 illustrates the angle of the velocity vectors for various nodes on the face of the free motion headform.

## Parameter Optimization

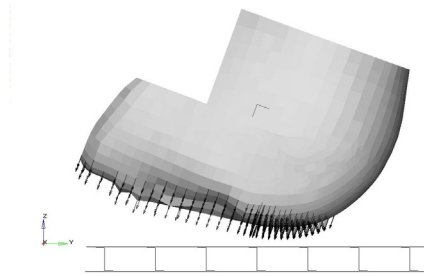


Figure 2. Angle of approach.

The successive response surface method (SRSM) [2] was used to determine the combination of three design factors - crush space, fin spacing, and fin/web/cover shell thickness - that would minimize the amount of crush space required in order to maintain  $HIC(d) < 700$ , in other words, to solve the optimization problem

minimize crush space

subject to the constraint that

$HIC(d) < 700$ .

The algorithm used here closely followed the default implementation of the successive response surface method (SRSM) as outlined in LS-OPT [5].

A sequence of linear response surfaces was used.  $3^3$  full factorial designs were defined to be the basis experiments for each of the response surfaces. D-optimal subsets - with seven combinations of each of the three design factors in each subset - were selected and used to define the set of simulations that were performed for the response surfaces.

After each set of finite element analyses was performed, regression coefficients were calculated based on the simulation results so that  $HIC(d)$  could be approximated as a linear function of crush space, fin spacing, and fin/web/surface shell thickness. Subsequently, the optimal combination of factor levels for each surface was determined by means of a simple sorting algorithm and used as the center point for the next iteration.

Once the new center point values for the objective function - crush space - and the design variables - crush space, spacing, and shell thickness were within 1% of those of the current iteration, the process was considered to have converged.

If convergence was not achieved subsequent to a particular iteration, the ranges for each of the design variables in the next iteration were calculated according to the algorithm outlined in [2] and [5], and the process was repeated.

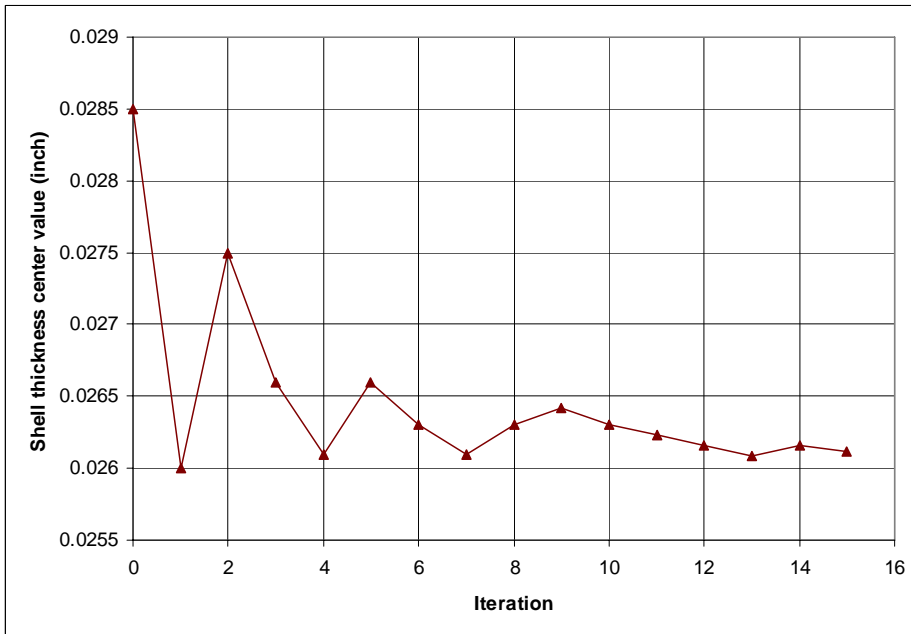


Figure 3. Convergence of shell thickness.

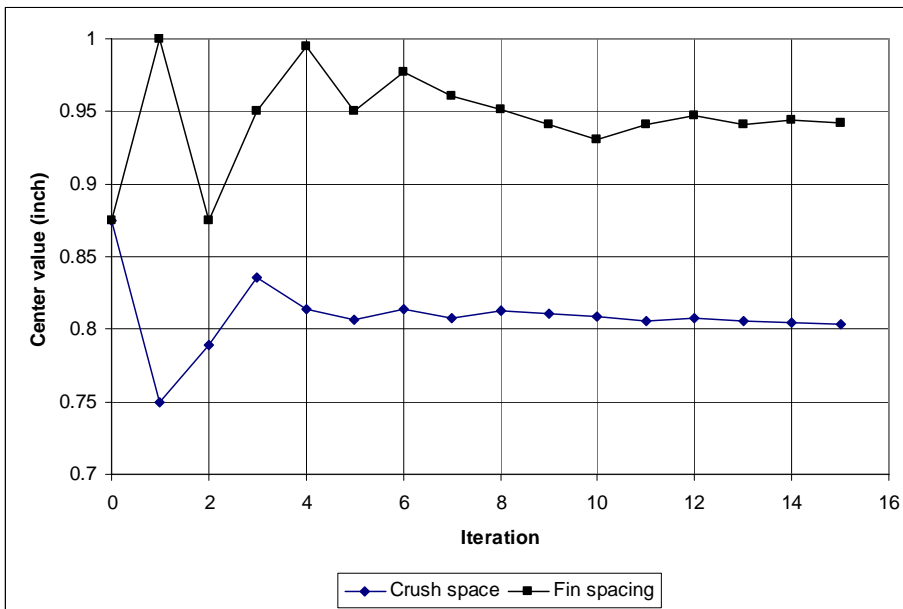


Figure 4. Convergence of crush space and fin spacing.

Convergence was quantitatively achieved after 15 iterations. The convergence of surface center point results is summarized in Figures 3 and 4 and in Table 1. It is evident from the results that the iteration process had, for the most part, converged to optimal levels after about ten iterations.

The minimum value of the objective variable – crush space – was determined to be about 0.80 inch for HIC(d) to be less than 700. A finite element simulation at the predicted optimum conditions produced a result of HIC(d) = 699.

	Initial	Optimum
Crush space (inch)	0.875	0.8044
Fin spacing (inch)	0.875	0.9446
Fin / web / cover shell thickness (inch)	0.0285	0.02616
HIC(d)	737	699

Table 1. Convergence of design input and output parameters.

The acceleration – time history exhibited by the optimum design is shown in Figure 5.

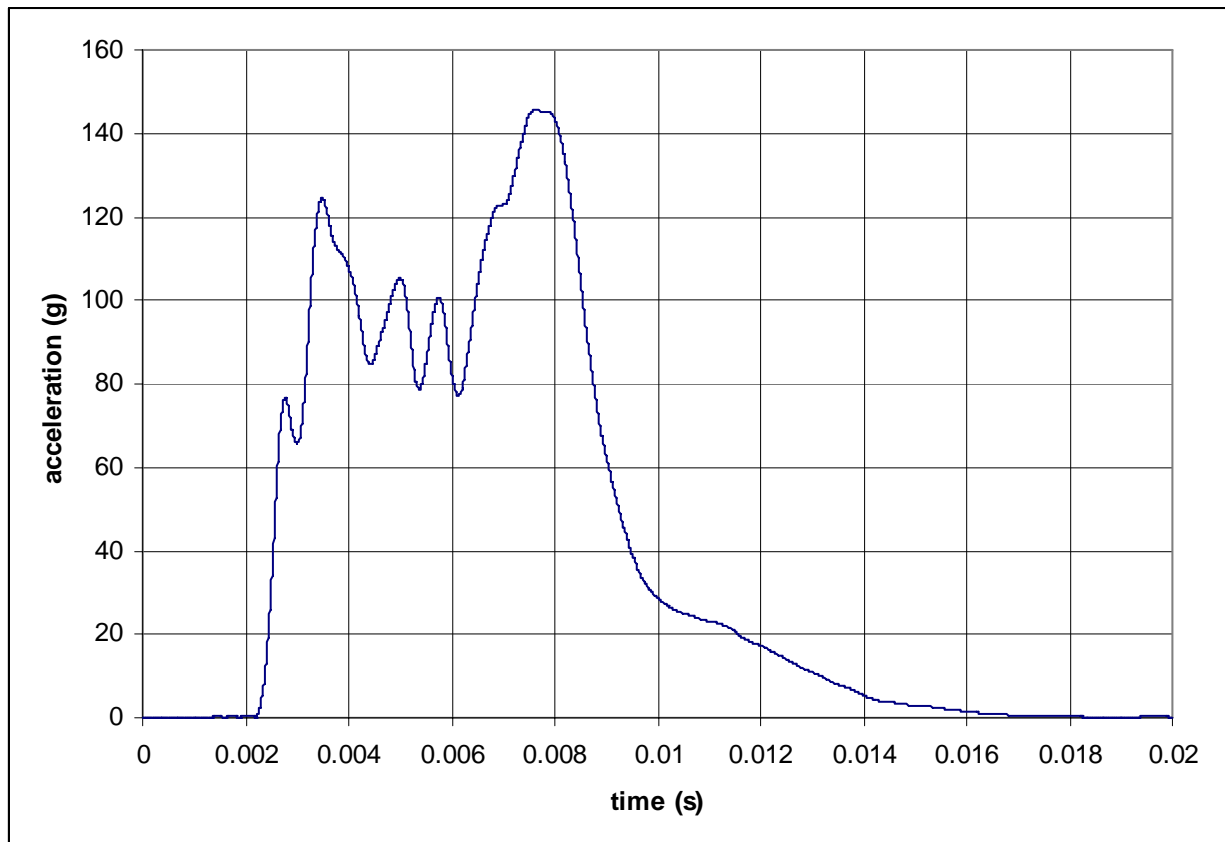


Figure 5. Acceleration – time history for optimum design.

### Robustness Analysis and Design Improvement

Once an optimum set of design parameters was found, an analysis was performed in order to estimate the degree to which HIC(d) performance of the device would be affected by moderate variations in crush space, web spacing, and shell thickness. Some degree of variability in HIC(d) response would be expected to result from typical manufacturing, assembly, and installation processes. An improved understanding of what might result as a result of this variability would be expected to help to ensure greater robustness in later product design iterations.

Myers and Montgomery [6] suggested a technique for investigating robustness involving analysis of the interactions between noise and input variables. They noted that interaction plots, based on classical factorial experimental methodology, can be used to estimate the effects of input variable interactions on the mean value and on the variability of output variables.

A classical 2<sup>3</sup> full factorial design with each of the design factors set to levels ±5% of optimum was used to develop interaction plots. A full factorial design was used because a half fraction would not offer sufficient resolution to prevent aliasing between first order interactions. A cube plot for the factorial design is shown in Figure 6.

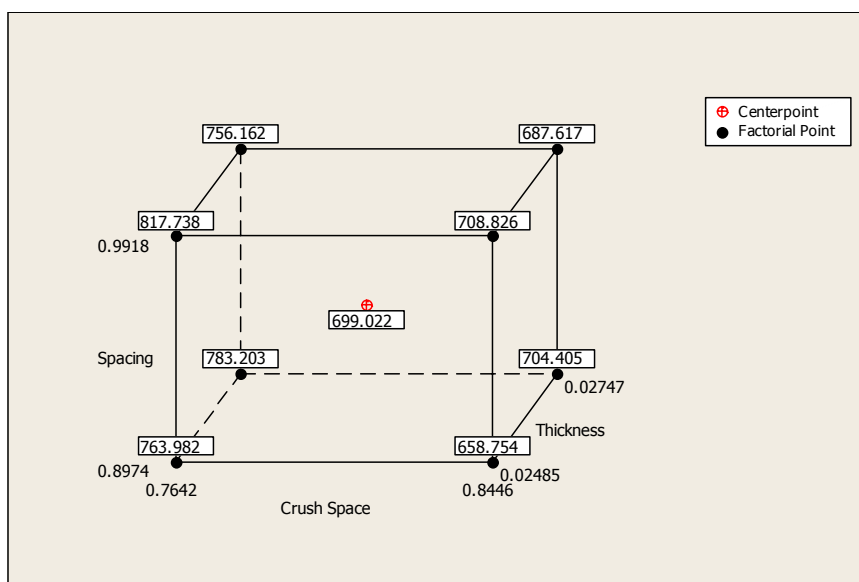


Figure 6. Results for factorial design.

Two of the design variable interactions were found to be significant – the interaction between crush space and shell thickness and the interaction between fin spacing and shell thickness (Figure 7). Of these two, the interaction between crush space and shell thickness was found to have a much more pronounced effect on HIC(d) response than the interaction between spacing and thickness. The variability of HIC(d) with changes in crush space is reduced somewhat at higher levels of shell thickness.

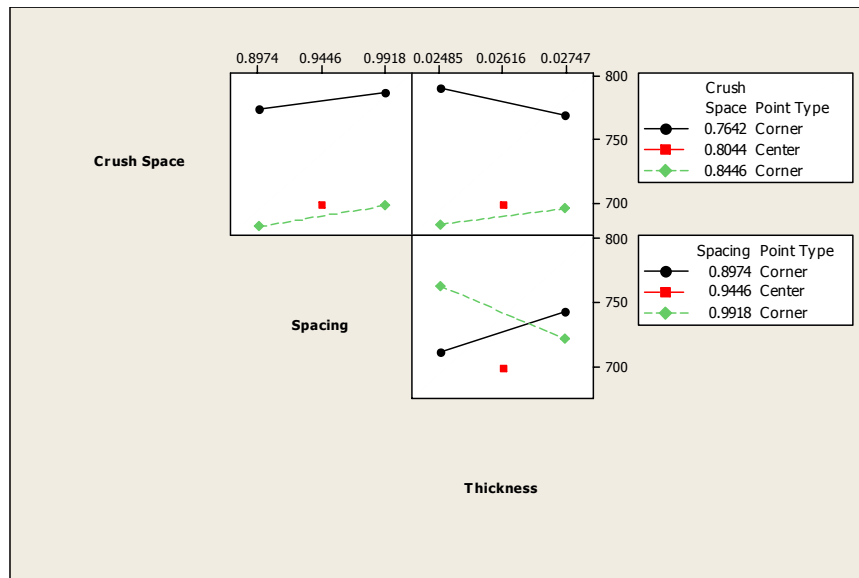


Figure 7. Interaction plot for crush space and shell thickness.

The crush space – shell thickness interaction is caused by the combination of two effects (Figure 8). A comparison of the deceleration peaks that occur at about 8 milliseconds indicates that the peaks for the devices with lower shell thickness were more severe. These peaks correspond to the increase of stiffness that is related to the onset of almost complete deflection of the energy absorber fins. The lower level of shell thickness reduces the amount of free motion headform kinetic energy transformed to absorber device internal strain energy during the fin buckling phase of the impact event. At the lower level of crush space, as the head exhausts the space available for deflection, impact severity becomes more pronounced as a result of increased mean deceleration due to reduced stopping distance.

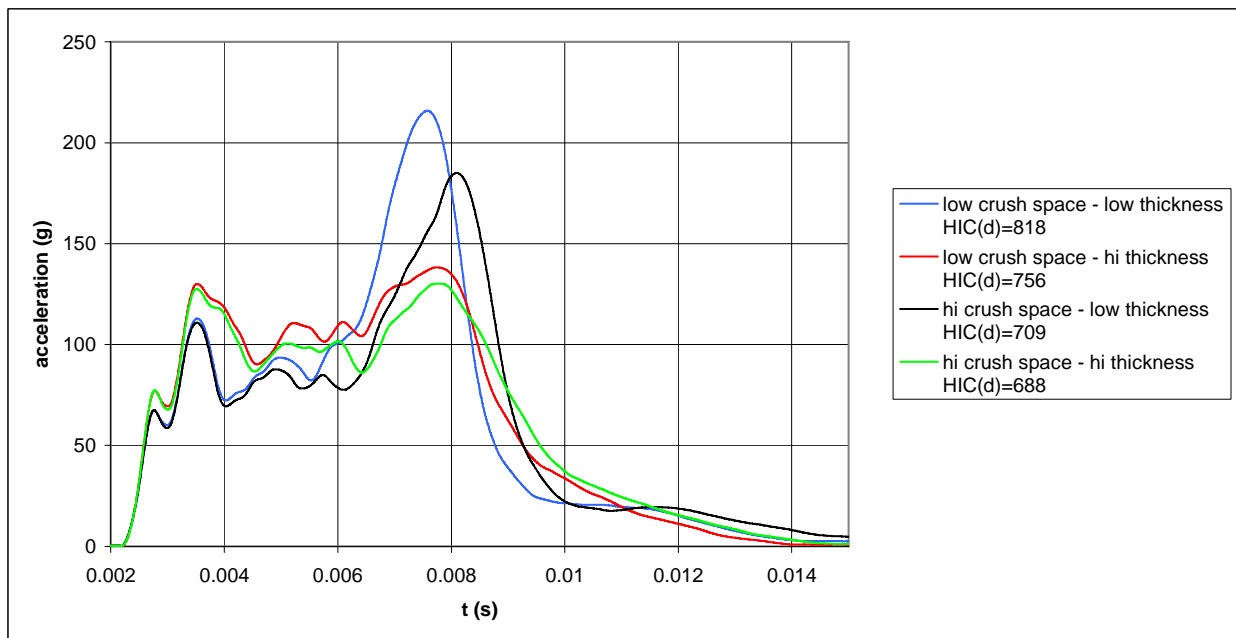


Figure 8. Interaction between crush spacing and shell thickness: acceleration vs. time histories.

At the higher level of shell thickness, the absorber transforms, during fin buckling, significantly more of the kinetic energy of the free motion headform into internal strain energy of the device. As a result the disparity between HIC(d) observed at the two levels of crush space is much less for the higher level of shell thickness than the disparity observed for the two crush space levels at the lower level of shell thickness.

An inspection of the 0.8446 inch crush space (optimum value +5%) face of the cube plot for the factorial design (Figure 6) revealed a possible opportunity for design improvement relative to the requirement that HIC(d) be less than 700. It was assumed, based on the results from the factorial design, that HIC(d) would decrease monotonically with increasing crush space and would probably, for values of crush space that were relatively close to 0.8446 inch, be minimized for values of spacing and shell thickness that were somewhere between the extreme values that were set in the factorial design. A linear interpolation technique was used to iteratively estimate a minimum value of crush space for which, given spacing fixed at 0.9918 inch and shell thickness set at 0.02485 inch, HIC(d) would be expected to be held to values less than 700.

Using this technique, a new value for nominal crush space less 5% was determined to be 0.8562 inch. A new 2<sup>3</sup> full factorial experiment was performed; the results appeared to show that given a new nominal value for crush space of 0.8975 inch – an increase of less than 0.01 inch over the original nominal value - the new design would indeed meet the criterion that HIC(d) be less than 700 (Figure 9) for nominal values ± 5%.

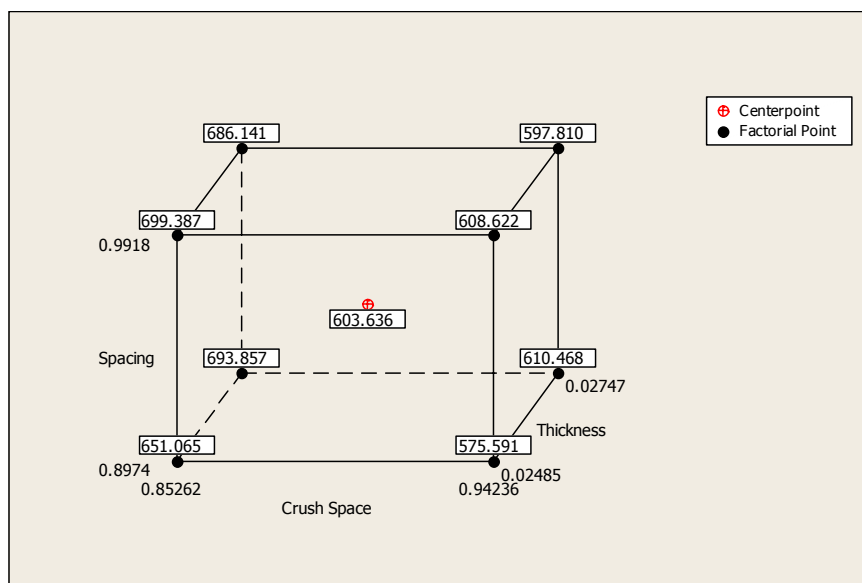


Figure 9. Factorial results for improved design.

Inspection of the interaction plots for the new design (Figure 10) reveals that, with the new design, there is very little interaction between crush space and shell thickness or crush space and spacing. There is still some interaction between spacing and shell thickness. Although an incremental improvement in robustness might be possible with an increase in thickness, it was

not pursued any further since the new design already meets the criterion of HIC(d) less than 700 for nominal values of design variables  $\pm 5\%$ .

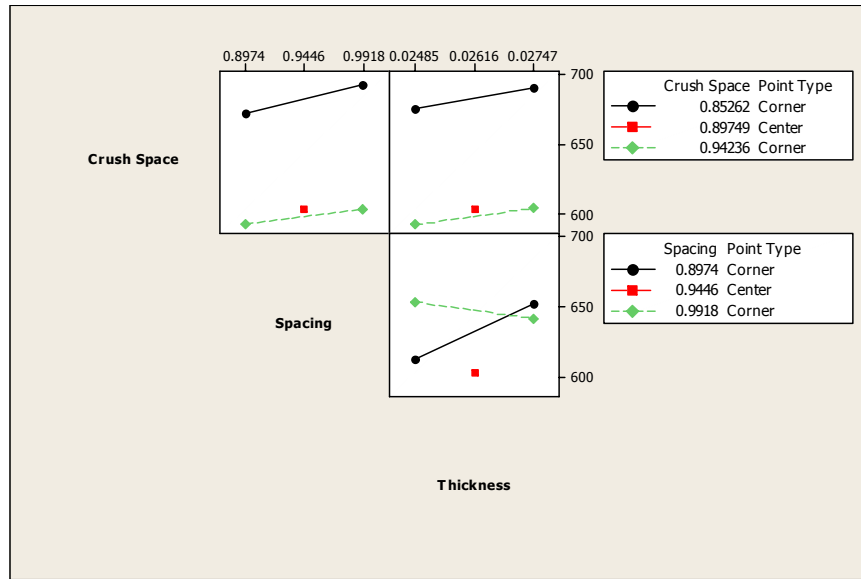


Figure 10. Interaction plots for improved design.

Further characterization of the behavior of the new design was achieved by development of a response metamodel. Comparative results reported by Simpson, Lin, and Chen [7] revealed that uniform designs would be a good choice for a space filling design and that Kriging would be an appropriate choice for the model used to generate a response surface. Uniform designs based on centered  $L_2$  discrepancy that were developed using the threshold accepting method [8] were acquired at <http://www.math.hkbu.edu.hk/UniformDesign/>.

Kriging models are of the form

$$\hat{y} = \sum_{k=1}^p \beta_k f_k(\bar{x}) + Z(\bar{x}) \quad (3)$$

The first term in the expression is a regression model; the second term is a model of a random process with mean zero and covariance

$$V(x_i, x_j) = \sigma^2 R(x_i, x_j) \quad (4)$$

where  $\sigma^2$  is the process variance and R is the correlation. A Gaussian spatial correlation function of the form

$$R(x_i - x_j) = \exp[-\theta(x_i - x_j)^2] \quad (5)$$

was used for the purposes of the current work. Kriging calculations were performed by means of the DACE MATLAB Kriging Toolbox which can be found at <http://www2.imm.dtu.dk/~hbn/dace/>. The technical report and manual [9] associated with this Toolbox give a detailed explanation of the calculations associated with development and use of a Kriging model.

A zero order polynomial – in other words, a constant - is often the regression term of choice for Kriging metamodels. Martin and Simpson [10] demonstrated and suggested the value of the use, at times, of higher order polynomials for improving Kriging metamodel approximation of deterministic computer models. Metamodels were, for the purposes of the work here, developed using uniform designs and with regression models comprised of a constant, of a linear polynomial, and of a quadratic polynomial.

Following Simpson, et. al. [7], two measures were used to attain relative estimates of goodness of fit for the metamodels. The first involved calculation of the root mean squared error (RMSE) between the Kriging estimate and the known, independent results generated earlier for the improved design via the  $2^3$  factorial design with a center point.

$$RMSE \equiv \left[ \sum_i \frac{(y_i - \hat{y}_i)^2}{n} \right]^{1/2} \quad (6)$$

The second measure involved calculation of the maximum error between the metamodel and the known points.

$$Maximum\ Error \equiv \max |y_i - \hat{y}_i| \quad (7)$$

Comparisons of the various combinations of sample size and regression model are given in Table 2 in terms of RMSE and in Table 3 in terms of maximum error. Due to the fact that even a simple quadratic regression model contains 10 terms it was clearly not possible to generate a Kriging metamodel with a quadratic regression for a sample size of 9.

Sample size	Constant	First Order Polynomial	Quadratic Polynomial
9	25.84	19.47	-
17	12.35	16.00	19.02
30	23.95	15.04	10.67

Table 2. RMSE comparison for various Kriging metamodels.

Sample size	Constant	First Order Polynomial	Quadratic Polynomial
9	42.70	29.52	-
17	23.84	37.44	34.92
30	53.39	30.08	18.66

Table 3. Maximum error comparison for various Kriging metamodels.

Although there were no clear trends, the metamodel that minimized these measures and seemed to thus best fit the known factorial results was the one generated with a quadratic polynomial and with a sample size of 30.

Results from that metamodel are represented in contour plots of HIC(d) vs. crush space and thickness for three different levels of spacing (Figures 11, 12, and 13). The ranges for the independent variables are 0.95-1.05. A value of 1.00 corresponds to the nominal value for the improved design; 0.95 and 1.05 correspond to values that are nominal less 5% and nominal plus 5%, respectively.

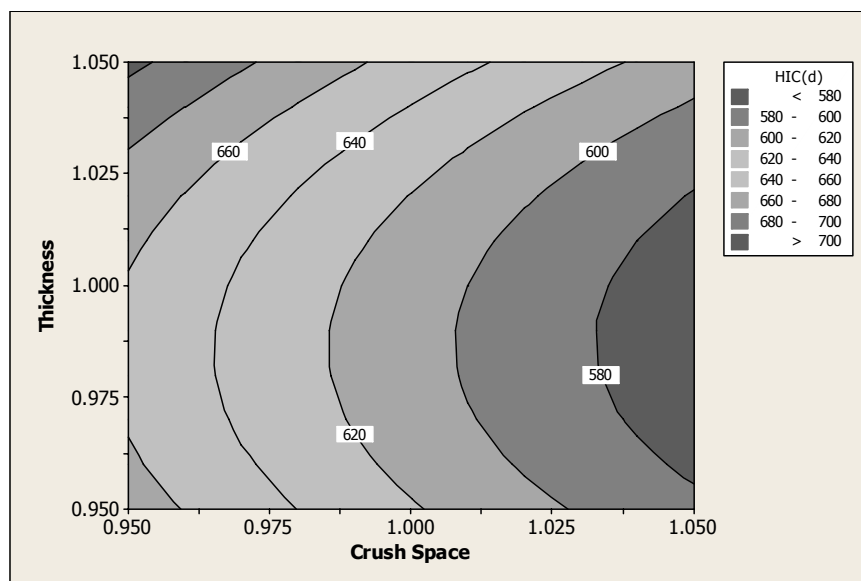


Figure 11. Contour plot for improved design, spacing = 0.95 (5% lower than nominal value).

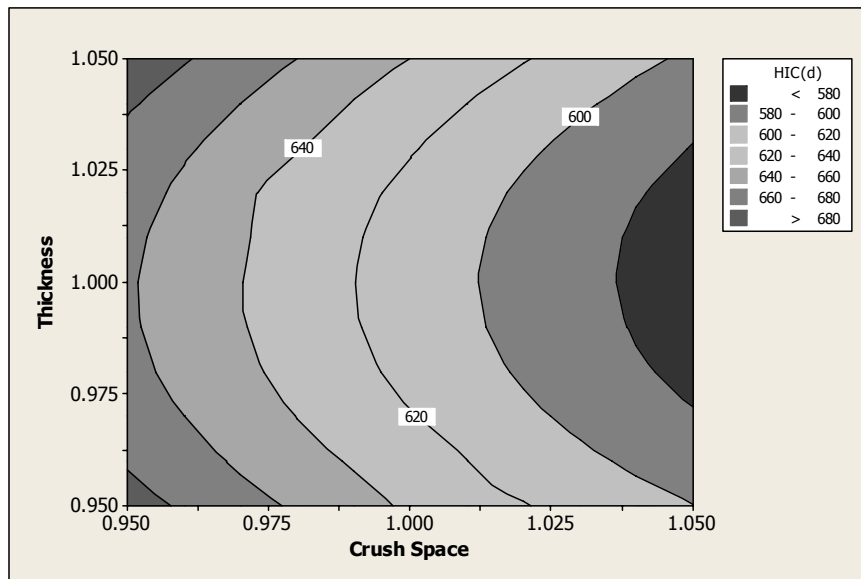


Figure 12. Contour plot for improved design, spacing = 1.00 (nominal value).

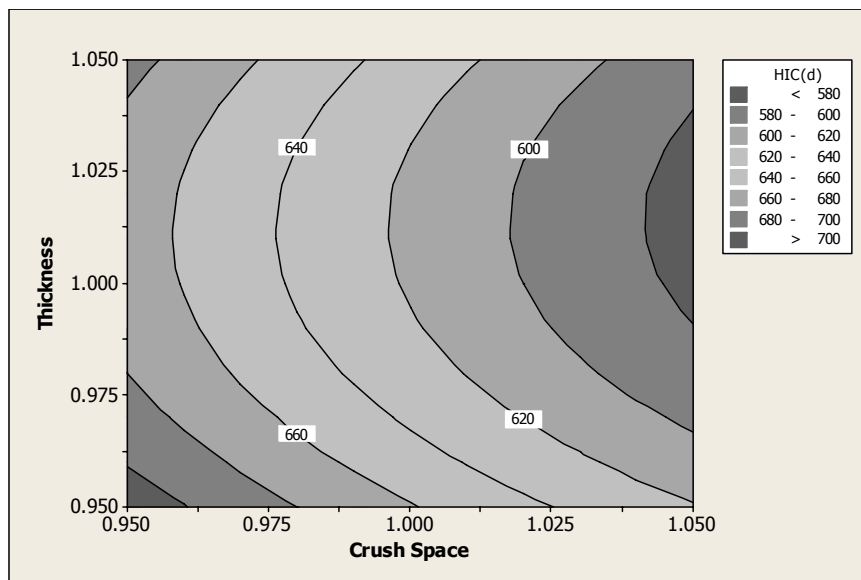


Figure 13. Contour plot for improved design, spacing = 1.05 (5% higher than nominal value).

Slight bias error between the Kriging metamodel and the known values from the factorial design caused contours that showed HIC(d) in excess of 700 near combinations of 0.95 crush space, 0.95 spacing, 1.05 shell thickness (Figure 11) and 0.95 crush space, 1.05 spacing, 0.95 shell thickness (Figure 13). Other than these moderate discrepancies, the metamodel appeared to support a thesis that HIC(d) for the improved design remained below 700 for the nominal design values  $\pm 5\%$ .

## Conclusions

It is possible to very efficiently optimize an energy absorber design using the LS-DYNA explicit finite element code in conjunction with the successive response surface method algorithm. Use of classic factorial techniques in combination with Kriging response surfaces can guide improvement of product robustness and offer insight into the nature of a product and its performance variability. An enlightened combination of these techniques enables, if nothing else, valuable and relatively inexpensive insight into the feasibility and behavior of various design concepts.

## References

- [1] Fox, D., Energy Absorber for Vehicle Occupant Safety and Survivability, Proceedings of the 17<sup>th</sup> Annual Ground Vehicle Survivability Symposium, Redondo Beach, CA, 2006.
- [2] Stander, N., Craig, K.J., On the robustness of a simple domain reduction scheme for simulation-based optimization, *Engineering Computations*, 19(4), pp. 431-450, 2002.
- [3] Livermore Software Technology Corporation (LSTC), LS-DYNA Keyword User's Manual, Version 970, Livermore, CA, 2003.
- [4] United States Code of Federal Regulations Title 49 (Transportation) Chapter V (NHTSA, DOT) Part 571 - 201U, Upper Interior Head Impact Protection.
- [5] Stander, N., Roux, W., Eggleston, T., Craig, K., LS-OPT User's Manual, Version 3.0, Livermore, CA, 2005.
- [6] Myers, R.H., Montgomery, D.C. *Response Surface Methodology. Process and Product Optimization using Designed Experiments*, Second Edition, Wiley, 2002.
- [7] Simpson, T., Lin, D., and Chen, W., Sampling Strategies for Computer Experiments: Design and Analysis. *International Journal for Reliability and Applications*, Aug. 2001 (Revised Manuscript).
- [8] Fang, K.T., C.X. Ma and P. Winker (2001). Centered  $L_2$ -discrepancy of random sampling and Latin hypercube design, and construction of uniform design, *Math. Computation.*, 71, 275-296.
- [9] Lophaven, S., Nielsen, H., Sondergaard, J., Technical Report IMM-TR-2002-12, DACE - A MATLAB Kriging Toolbox, Version 2.0, Lyngby, Denmark, 2002.
- [10] Martin, J. and Simpson, T., Use of Kriging Models to Approximate Deterministic Computer Models, *AIAA Journal*, 43(4), pp. 853-863, 2005.

